

EMBEDDABLE MICROINSTRUMENTS FOR CORROSION MONITORING

R. G. Kelly<sup>1</sup>, J. Yuan<sup>1</sup>, S. H. Jones<sup>2</sup>, W. Blanke<sup>2</sup>, J. H. Aylor<sup>2</sup>, W. Wang<sup>2</sup>, A. P. Batson<sup>3</sup>  
Departments of Materials Science and Engineering<sup>1</sup>, Electrical Engineering<sup>2</sup>, Computer Science<sup>3</sup>  
School of Engineering and Applied Science  
University of Virginia  
Charlottesville, VA 22903

A. Wintenberg  
Instrumentation and Control Division  
Oak Ridge National Laboratory  
Oak Ridge, TN 37831-6006

G. G. Clemeña  
Virginia Transportation Research Council  
Charlottesville, VA 22903

ABSTRACT

The design and development of an embeddable corrosion measurement microsystem which takes advantage of the increased availability of Application Specific Integrated Circuit (ASIC) development and Very Large Scale Integrated (VLSI) circuit manufacturing is described. Key elements of the system (micropotentiostat with zero resistance ammeter (ZRA) and analog-to-digital (A/D) and digital-to-analog (D/A) converters were tested electronically and found to perform satisfactorily. The micropotentiostat/ZRA combination was also tested on steel electrodes exposed to 0.6 M NaCl, saturated Ca(OH)<sub>2</sub>, and saturated Ca(OH)<sub>2</sub> + 0.6 M NaCl. Comparisons of polarization resistance data generated by the micropotentiostat and commercially available systems demonstrated that the two systems performed equivalently. The 10-bit A/D and 6-bit D/A converters exhibited excellent linearity over a wide range of inputs. Future directions for the development of the embeddable corrosion measurement microsystem are also outlined.

Keywords: corrosion monitoring, polarization resistance, corrosion rate, instrumentation, microsystem, steel

Copyright

## INTRODUCTION

The high costs and complexity of corrosion place ever-increasing demands on corrosion monitoring systems. Costs are driven by increasing industrial competitiveness as well as environmental concerns. Competitiveness requires minimization of operational costs, including downtime due to unexpected corrosion failures. Increased concern about environmental contamination has required all industries to implement accurate, but cost-effective, corrosion monitoring methods. However, the complexity of different types of corrosion complicates corrosion monitoring. The temperature as well as the concentrations of dissolved species (*e.g.*, pH, [Cl<sup>-</sup>]) dramatically affect both the type of corrosion and its rate. The controlling parameters can fluctuate with time, requiring frequent, real-time measurements.

A complete corrosion measurement system must be capable of making accurate measurements not only of electrochemical parameters related to corrosion rate (*e.g.*, polarization resistance), but also simultaneously other important environmental parameters such as pH, temperature, chloride ion concentration, and conductivity. The operator (or ideally, the system) could then use all this information to assess the situation and make a fully informed decision concerning what mitigation strategies, if any, to apply. Thus, a complete corrosion measurement system would have a high-level design as shown in Figure 1 and would contain the following components:

- (a) one or more sensors (*e.g.*, for electrochemical measurements of corrosion, pH, temperature, chloride ion concentration, conductivity),
- (b) a potentiostat with an autoranging zero resistance ammeter (ZRA) for electrochemical measurements,
- (c) high input impedance amplifiers for the various sensors,
- (d) analog-to-digital (A/D) and digital-to-analog (D/A) converters,
- (e) a microprocessor capable of controlling the electrochemical measurements, managing the measurements from the sensors, integrating the information from the various sensors into an intelligent assessment of the corrosion situation, and communicating with the external world,
- (f) a means of communicating with the external world via either a serial communications port or microwave telemetry,
- (g) a reliable power source.

Such systems are commercially available. However, these systems are composed of individual instruments, each of which is on the size scale of tens of centimeters. When combined, the measurement system often has a size on the order of 1 meter.

### Need for Embeddable Microinstruments

In many corrosion monitoring applications, strict constraints are imposed on the size of the monitoring equipment. Such constraints often preclude the monitoring of key structures by conventional corrosion monitoring systems. For example, in the corrosion monitoring of the reinforcing bars in bridge decks, the need to spatially map variations in the corrosion rate puts limits on the size of the probes to be used. In addition, direct measurement of corrosion rate is highly desirable, as opposed to indirect measurements such as external potential mapping or concrete conductivity. High installation expense represents an additional constraint on corrosion monitoring of extensive structures such as bridges, aircraft, chemical plants, and pipelines. Commercially available systems made of large, discrete instruments are not well-adapted to the introduction of a large network of independent corrosion

monitoring systems. In some instances, it would be advantageous if the entire microsystem were embeddable. Monitoring of corrosive conditions in reinforced concrete or on off-shore structures represent two cases in which the need to have the measurement system physically tethered to an external site (e.g., a data logger or computer) prevents aggressive corrosion monitoring. The limitations on system reliability for such arrangements and the difficulty in sealing the sites at which the tethering cables emerge from the structure can be key hurdles in the implementation of real-time corrosion monitoring in such applications.

## Design Philosophy

In order to overcome the limitations of commercially available corrosion monitoring approaches, the recent advances in the availability of Application Specific Integrated Circuits (ASIC) and very large scale integration (VLSI) manufacturing have been exploited to design embeddable corrosion microsystems. These microsystems will have all of the characteristics listed above. Their physical footprint will be on the order of several millimeters to a centimeter. By exploiting the mass production capabilities inherent in monolithic microelectronic fabrication techniques, these systems should be able to be produced at very low unit cost. This paper discusses the progress to date on the design and fabrication of such embeddable microinstrument systems and the results of testing of some key components.

## EXPERIMENTAL

### VLSI Design and Implementation of the Microinstrument

The Metal Oxide Semiconductor Implementation Service (MOSIS) acts as a clearinghouse that accepts computer-aided designs of integrated circuits and implements them through the VLSI manufacturing process for U.S. universities and small businesses. All of the components discussed in the present work were designed according to the rules for a 2.0  $\mu\text{m}$ , double polysilicon, analog/digital CMOS process. Two VLSI designs were submitted. Figure 2 shows the first design which consisted of a  $2.2 \times 2.2$  mm chip containing eight operational amplifiers. This chip was used to test the micropotentiostat/zero resistance ammeter concept. Six copies of this chip were returned in 40 pin dual-inline-packages. Figure 3 shows the second design which contained three on-chip electrodes for electrochemical measurements, as well as analog integrated circuits for amplification and signal conditioning, A/D and D/A conversion and a micropotentiostat with an autoranging ZRA on a  $4 \times 6$  mm chip. The latter design was returned in 64 pin standard packages. This package configuration was chosen in order to facilitate testing of the individual components.

### Circuit Testing

Each of the components was tested individually to determine performance characteristics using conventional electrical characterization methods, details of which are available elsewhere<sup>1</sup>. The micropotentiostat/ZRA combination was tested as a standalone device using the configuration shown in Figure 4. Stepwise, potentiostatic polarization resistance measurements were made (5 mV or 100 mV steps, 30 s step time) on off-chip dummy cells as well as actual corroding systems. The dummy cell studied was a combination of a  $1\text{k}\Omega$  resistor in parallel with a  $47 \mu\text{F}$  capacitor, with this parallel combination in series with a  $1 \text{ k}\Omega$  and a  $2 \text{ k}\Omega$  resistor as also shown in Figure 4. All resistors had a 1% tolerance. The 6-bit D/A converter was tested with a circuit containing a 6 line DIP switch with pull up

resistors which provided the digital input signals. The 10-bit, successive approximation A/D converter was tested with a custom-fabricated board that generated the required signals for the A/D controller as well as the analog signal to be converted. The output of the A/D converter was connected to a logic analyzer.

Electrochemical testing was performed on carbon steel samples ( $4.9 \text{ cm}^2$ ) immersed in 0.6 M NaCl, saturated  $\text{Ca}(\text{OH})_2$ , or saturated  $\text{Ca}(\text{OH})_2 + 0.6 \text{ M NaCl}$ . Polarization resistance measurements were conducted in the same manner as with the dummy cell. The polarization resistance value was calculated from the resulting current/voltage curves via linear regression. The results from the micropotentiostat were compared to results from commercially available electrochemical corrosion measurement systems.

## RESULTS AND DISCUSSION

### Dummy Cell Results

Table 1 lists some of the basic operating characteristics of the operational amplifiers which comprise the micropotentiostat/ZRA and which will be used as amplifiers for other sensors as well. Potentiostatic polarization curves developed for the dummy cell are shown in Figures 5 and 6. Figure 5 shows the results from a scan from -0.1 V to +1.1 V in 100 mV steps. The two curves represent data using either the applied voltage,  $V_{in}$ , or the voltage measured between the WE and RE connections,  $V_R$ . Excellent linearity was observed between the applied current and both  $V_{in}$  and  $V_R$ . Regression analyses gave values of 2008 and  $1963\Omega$  for the data using  $V_R$  and  $V_{in}$ , respectively. These values compare within 1.2% of the actual value of the DC resistance of the dummy cell of  $1985\Omega$ . A small offset was observed between  $V_{in}$  and  $V_R$ , amounting to 10 mV at an applied voltage of 1 V. These values cover virtually the entire range of corrosion potentials of most engineering materials.

The accuracy of the micropotentiostat for small amplitude measurements such as polarization resistance was also assessed. Potentiostatic polarization measurements were also made over  $\pm 20 \text{ mV}$  using 5 mV steps as shown in Figure 6. Linear regression analyses gave values of 2018 and  $1962\Omega$  for  $V_R$  and  $V_{in}$ , respectively, which are within 1.7% of the actual value. The correlation coefficient was 0.9992. For comparison, the same experiments were conducted with a commercial corrosion measurement system. The resistance value from these data was  $1992\Omega$ , with a correlation coefficient of 1.0. Thus, the microinstrument performs very well even for small amplitude measurements.

### Electrochemical Testing Results

Figures 7 and 8 compare the results of polarization resistance tests on carbon steel exposed to 0.6 M NaCl at room temperature as measured by a commercial potentiostat and the micropotentiostat. The commercial potentiostat was controlled by commercially available software and measured the polarization resistance using the potential staircase method outlined above. A polarization resistance of  $3.13 \text{ k}\Omega\text{-cm}^2$  was calculated from the data (Figure 7), with a correlation coefficient of 0.971. The microinstrument data (Figure 8) generated a value of  $R_p$  of  $3.42 \text{ k}\Omega\text{-cm}^2$ , with a correlation coefficient of 0.999. The potential reported for the microinstrument was that measured between the working and reference electrodes. Using a value of 0.021 V for the B factor in the Stern-Geary relationship<sup>2</sup>:

$$i_{corr} = \frac{B}{R_p}$$

yields a corrosion rate of  $6 \mu\text{A}/\text{cm}^2$  (2.8 mpy), a quite reasonable value for steel in salt water<sup>3,4</sup>.

The results of the polarization resistance measurements made on steel in saturated  $\text{Ca}(\text{OH})_2$  and saturated  $\text{Ca}(\text{OH})_2 + 0.6 \text{ M NaCl}$  measured by the microinstrument and by the commercial apparatus are shown in Table 1. Again, excellent agreement in the measurement of  $R_p$  between the two measurement systems was obtained ( $201 \text{ k}\Omega\text{-cm}^2$  by the micropotentiostat vs.  $194 \text{ k}\Omega\text{-cm}^2$  by the commercial system). These polarization resistances would correspond to a corrosion rate of approximately  $0.1 \mu\text{A}/\text{cm}^2$ , which is in excellent agreement with that expected for steel in this solution<sup>5,6</sup>. In a solution of saturated  $\text{Ca}(\text{OH})_2 + 0.6 \text{ M NaCl}$ , the polarization resistance was much lower, indicating more rapid corrosion. This change was detected by both the micropotentiostat ( $R_p = 7.7 \text{ k}\Omega\text{-cm}^2$ ) and the commercial system ( $R_p = 8.8 \text{ k}\Omega\text{-cm}^2$ ). It should be noted that the measurement was made first with the commercial instrument, indicating that the corrosion rate was increasing with time, as would be expected. These results demonstrate that the microinstrument is capable of measuring corrosion rates over a wide dynamic range.

### D/A and A/D Converter Testing

The results from the testing of the 6-bit D/A converter are shown in Figure 9. Excellent linear behavior is observed. The curve is also monotonic due to the choice of a resistor ladder network as the conversion scheme. This circuit will provide accurate conversion of data signals from the microprocessor to the input of the micropotentiostat for electrochemical testing. The results from the testing of the 10-bit, successive approximation A/D converter are shown in Figure 10. Again, excellent linear behavior is observed as shown by the high correlation coefficient of 0.999.

## CONCLUSIONS AND FUTURE PROSPECTS

This work has demonstrated the viability of producing the components necessary for a microsystem capable of making electrochemical measurement of corrosion rate using VLSI circuit design and manufacturing. Much remains to be explored to complete the development of a complete corrosion measurement system. The next stage of work will involve refining the micropotentiostat/ZRA circuit to improve performance by reducing offset voltage and offset current errors while adding autoranging capability to the ZRA. As indicated above, the autoranging ZRA has already been implemented into silicon. In separate work, several other useful components have been designed and implemented into silicon, including a 11-bit microprocessor, microwave power and input/output telemetry circuits, and a temperature sensor<sup>7</sup>. When combined, these components will form the basis for a complete measurement system. The microprocessor will be able to control the micropotentiostat, implement current interruption for automatic IR correction, manage input/output chores, and integrate the information from other available sensors. Other issues to address include the choice of packaging for long-term integrity and an investigation of power source options including remote power supplied via electrical connections, on-package power supplied from a battery, and remote power provided by inductive coupling via RF radiation.

## ACKNOWLEDGMENTS

Financial support from the Virginia Transportation Research Council, the National Science Foundation (CDA-8922545) and the Virginia Center for Innovative Technology is gratefully acknowledged.

## REFERENCES

1. W. Blanke, "Mixed-Signal and Sensor Components for the Design of Integrated Circuit Microinstruments," M.S. Thesis, Department of Electrical Engineering, University of Virginia, Charlottesville, VA (May, 1996).
2. M. Stern, A.L. Geary, *J. Electrochemical Soc.*, 104, (1957): p. 56.
3. S. Dexter, *ASM Handbook*, Vol. 13 Corrosion (American Society for Metals, Metals Park, OH, 1987), p. 898.
4. M. G. Fontana, N. D. Greene, *Corrosion Engineering* (McGraw-Hill, New York, (1978), p. 269.
5. C. M. Hansson, B. Sørensen, *Corrosion Rates of Steel in Concrete*, ASTM STP 1065 (N. S. Berke, V. Chaker, D. Whiting, eds., Amer. Soc. for Testing and Materials, Philadelphia, 1990), p. 3.
6. N. S. Berke, D. F. Shen, K. M. Sundberg, *Corrosion Rates of Steel in Concrete*, ASTM STP 1065 (N. S. Berke, V. Chaker, D. Whiting, eds., Amer. Soc. for Testing and Materials, Philadelphia, 1990), p. 38.
7. Z. K. Salman, S. H. Jones, R. M. Weikle, J. H. Aylor, *An Integrated, Wireless Microinstrument for Monitoring Skin Temperature*, Proc. of IEEE Intl. ASIC Conference, 9th Annual Meeting, (Rochester, NY, Sept. 1996).

TABLE 1  
OPERATING CHARACTERISTICS OF ORNL OPERATIONAL  
AMPLIFIER USING A 5 V POWER SUPPLY

Characteristic	Condition	Typical
Operating Range		1 to 4 V
Voltage Gain		10,000
Offset Voltage	Unity Gain	$\pm 50$ mV
Small Signal Bandwidth	Unity Gain	2 MHz
Slew Rate	3 V Pulse	4 V/ $\mu$ s
Full Power Bandwidth	3 V Pulse	425 kHz
Supply Current	10 k Bias Resistor	1.6 mA
Power Consumption	10 k Bias Resistor	8 mW

TABLE 2  
POLARIZATION RESISTANCES OF STEEL MEASURED WITH A  
COMMERCIAL SYSTEM AND THE MICROPOTENTIOSTAT

Solution Composition	Measured Polarization Resistance( $k\Omega\text{-cm}^2$ )	
	Commercial System	Micropotentiostat
saturated $\text{Ca}(\text{OH})_2$	194	201
saturated $\text{Ca}(\text{OH})_2 + 0.6 \text{ M NaCl}$	8.8	7.7

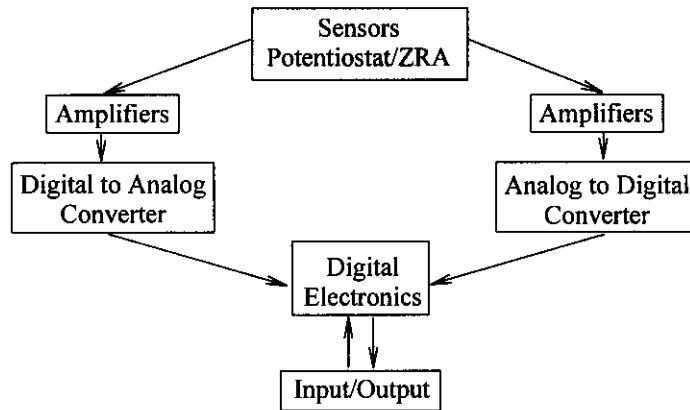


FIGURE 1 - Schematic representation of a complete corrosion measurement system consisting of sensors and associated amplifiers, potentiostat, A/D and D/A converters, microprocessor, communication circuitry.

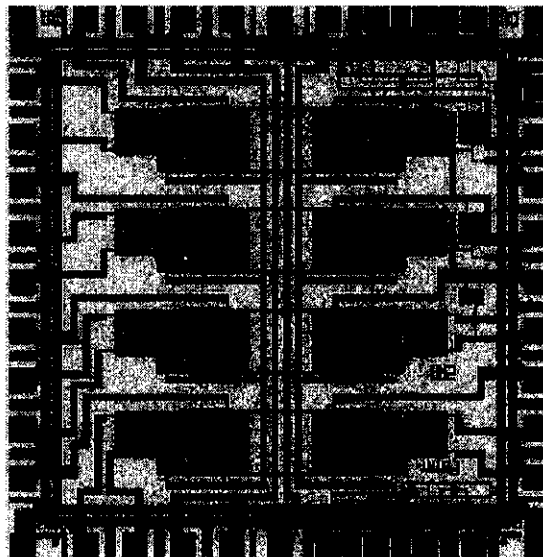


FIGURE 2 - First VLSI design containing eight operational amplifiers. The chip had dimensions of  $2.2 \times 2.2$  mm. Two of the operational amplifiers were used to form a potentiostat/ZRA combination.

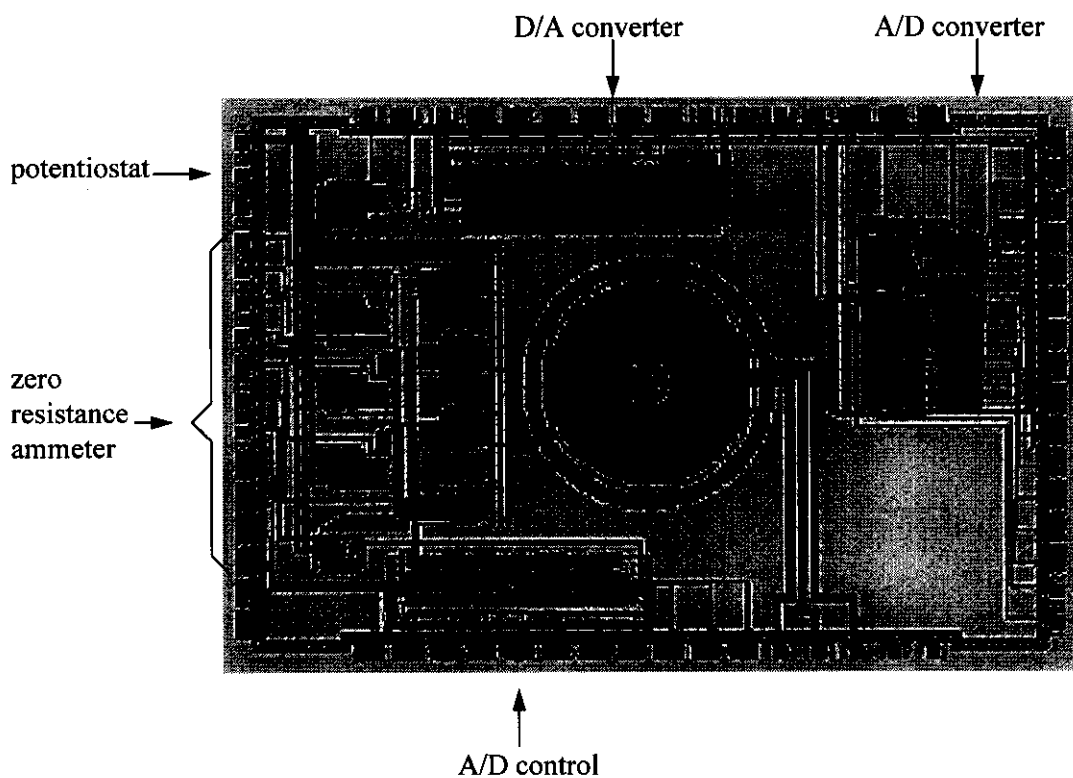


FIGURE 3 - Second VLSI design containing an integrated potentiostat/autoranging ZRA, A/D and D/A converters, and three on-chip electrodes.

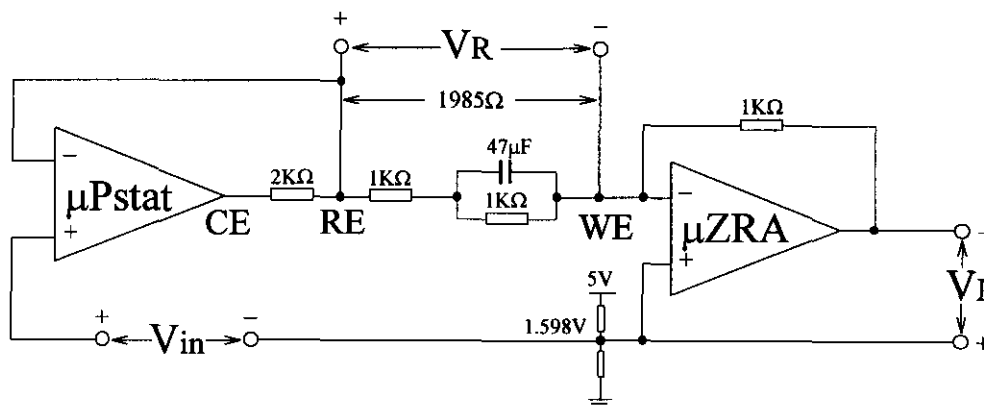


FIGURE 4 - Configuration of micropotentiostat/ZRA used for testing of operational amplifiers from first VLSI design, as well as the dummy cell used. The DC resistance of the dummy cell was  $1985\Omega$ .

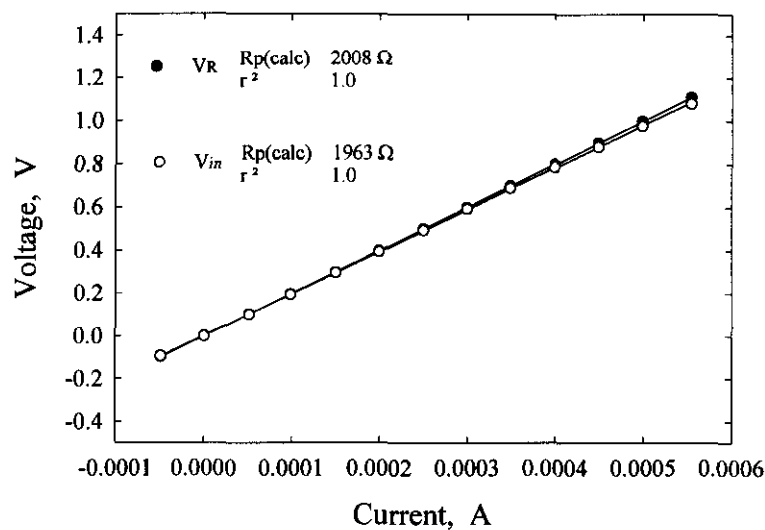


FIGURE 5 - Results from potentiostatic polarization using micropotentiostat with 100 mV step size, 30 s step time over a wide voltage range. Data are shown using both  $V_{in}$ , the applied voltage, and  $V_R$ , the measured voltage between the working and reference electrode connections. Results from regression analyses are also shown.

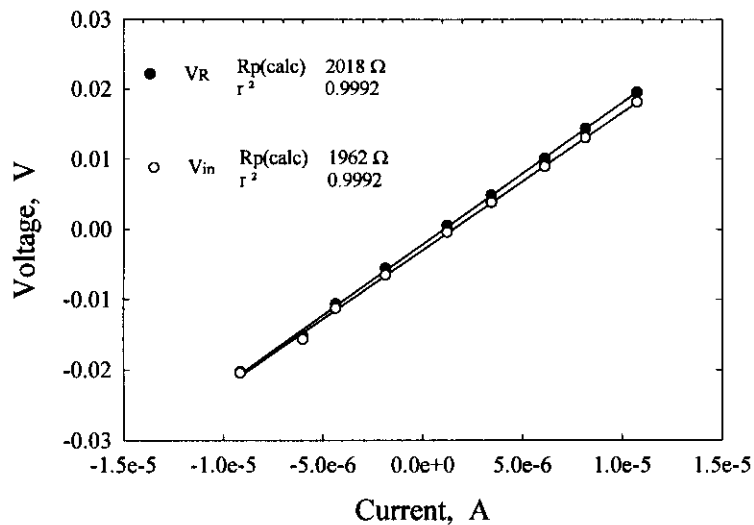


FIGURE 6 - Results from potentiostatic polarization using micropotentiostat with 5 mV step size, 30 s step time over a narrow voltage range. Data are shown using both  $V_{in}$ , the applied voltage, and  $V_R$ , the measured voltage between the working and reference electrode connections. Results from regression analyses are also shown.

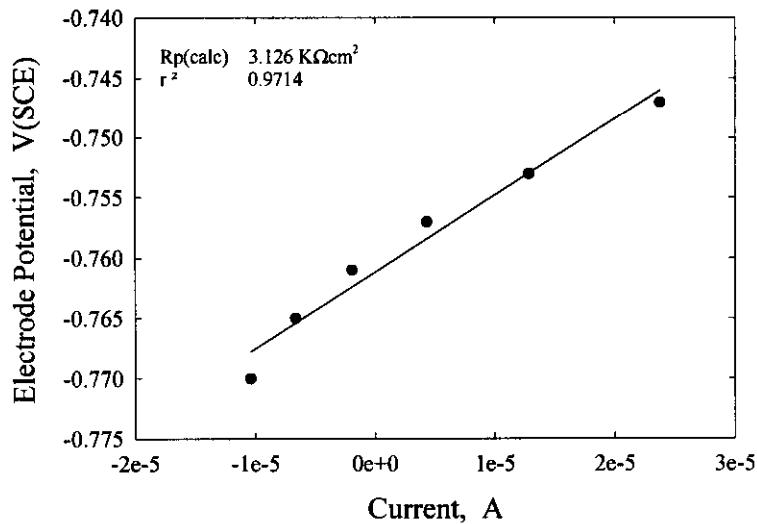


FIGURE 7 - Polarization resistance results for carbon steel exposed to quiescent 0.6 M NaCl using a commercial measurement system. Regression analysis gave value of  $R_p$  of  $3.13 \text{ k}\Omega\text{-cm}^2$  with a correlation coefficient of 0.971.

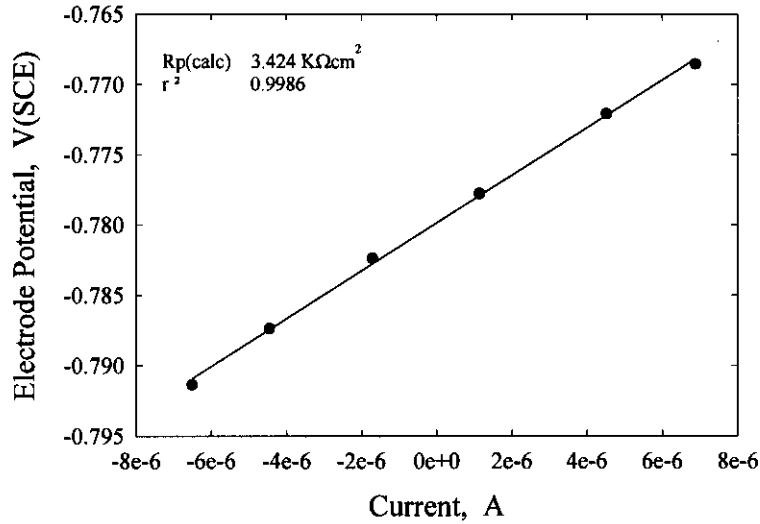


FIGURE 8 - Polarization resistance results for carbon steel exposed to quiescent 0.6 M NaCl using the micropotentiostat/ZRA combination. Regression analysis gave value of  $R_p$  of  $3.42 \text{ k}\Omega\text{-cm}^2$  with a correlation coefficient of 0.999.

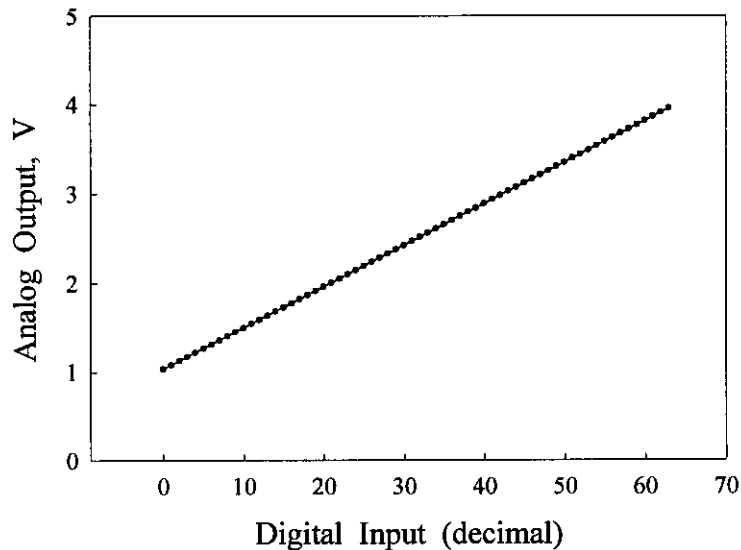


FIGURE 9 - Results from testing of D/A converter (6-bit digital input). Correlation coefficient from linear regression analysis was 1.0.

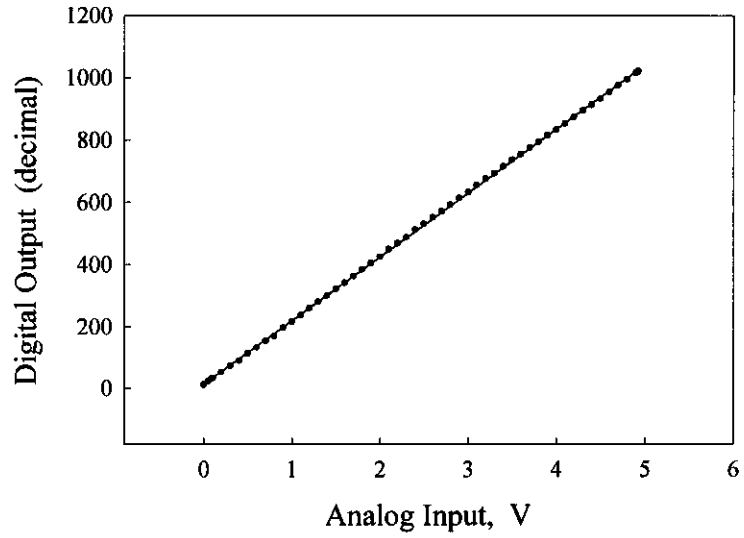


FIGURE 10 - Results from testing of successive approximation A/D converter (10-bit digital output). Excellent linearity is observed as evidenced by correlation coefficient of 0.999.